Correlations between nano-scale chemical- and polar-order in relaxor ferroelectrics and the length scale for polar nano-regions

B.P. Burton and Eric Cockayne[1] and U. V. Waghmare[2]

[1]*Ceramics Division, Materials Science and Engineering Laboratory, National Institute of Standards and Technology Gaithersburg, MD 20899-8520*

[2]*J. Nehru Theoretical Sciences Unit, JNCASR, Jakkur, Bangalore, 560 064, INDIA*

preprint; submitted to Physical Review Letters September 4, 2004; resubmitted

Large scale molecular dynamics simulations of a first-principles Hamiltonian for the model relaxor ferroelectric, $Pb(Sc_{1/2}Nb_{1/2})O_3$, were used to determine the nature of correlations between short-range chemical- and polar nano-regions that are thought to be essential to the glassy low-T behavior exhibited by some relaxors. Relative to chemically disordered regions (CDR), chemically ordered regions (COR) exhibit enhanced polarization, and polarization-fluctuations at all temperatures. Magnitudes of pairwise cluster-cluster polarization correlations follow the trend: COR-COR- ¿ COR-CDR- ¿ CDR-CDR-correlations. This result implies that the characteristic length-scale for polar nano-regions is the same as that for chemical short-range order.

PACS numbers: 77.80.Bh, 82.35.Jk, 83.10.Rp, 07.05.Tp, 61.43.Bn

Perovskite-based $A(B_{1/2}B'_{1/2})O_3$ and $A(B_{1/3}B'_{2/3})O_3$ relaxor ferroelectrics (RFE) [1, 2], such as $Pb(Mg_{1/3}Nb_{2/3})O_3$ (PMN) and $Pb(Sc_{1/2}Nb_{1/2})O_3$ (PSN), are technologically important transducer/actuator materials with extraordinary dielectric and electromechanical properties. They also exhibit fundamentally interesting Vogel-Fulcher [3] temperature (T) and frequency (ω) dependence of their dielectric constant, $\epsilon(T,\omega)$, that is not observed in conventional ferroelectrics (FE) or antiferroelectrics (AF)[4]. In RFE, $\epsilon(T,\omega)$ exhibits a broad peak that is associated with ω-dispersion, $1Hz \lesssim \omega \lesssim GHz$, which clearly indicates relaxation processes at multiple time-scales. While the oxymoronic phrase "diffuse phase transition" (DPT) is often used to describe RFE, they are distinct from other FE with a DPT, such as $Pb(Fe_{1/2}Nb_{1/2})O_3$, whose dielectric response does not have Vogel-Fulcher form [5]. The maximum temperature for an RFE is called the Burns temperature, T_{Burns}, and below T_{Burns} index of refraction data deviate from a Curie-Weiss trend. The minimum temperature is either a point of transition to a FE phase, as occurs in PSN, or a glassy freezing point, T_f, as occurs in PMN [6]. Some reserve the term RFE for systems such as PMN that have a T_f at low-T [6].

Fluctuations of the chemical short-range order (SRO) on a length scale of $\approx$ 2-6 nm[7–9] (5-15 unit cells) define nano-scale[10] heterogeneities with disordered local fields ($\vec{h}$) that are typically called random fields (RF) citeWestphal, Quian. Coupling between RF and FE degrees of freedom are thought to generate polar nanoregions (PNR) with collective dipole moments[13, 14], and PNR are deemed essential to the ferroglass freezing that is observed in PMN [6]. Elucidating the relationship(s) between chemical SRO, and PNR, and their respective length scales, is a long-standing and central problem in RFE-studies, and it is the primary focus of this Letter. In 1983, Burns and Dacol [13] suggested that polar clusters would be *"...several unit cells in size..."* whereas in 2003, Blinc et al. [6] describe them as *"...smaller than* 500 *Å.."* an uncertainty-range of ≈ 1.5 orders of magnitude.

The simulations described below link atomistic first principles calculations to mesoscopic models, such as the spherical random bond random field model (SRBRFM) [15]. A realistic microstructure (PSN [8], PMN[7, 9]) is modeled and analysed by directly calculating polarizations and dielectric suseptibilities for nano-scale chemically ordered regions (COR) in a percolating disordered matrix (PDM) of chemically disordered regions (CDR). Simulations allow a complete *spatial* analysis of correlations between chemical- and polar-ordering which has not been achieved experimentally, and therefore an analysis of the characteristic PNR length scale.

Simulations were performed for PSN rather than PMN because the PSN cation ordered ground-state is known, and this simplifies derivation and fitting of the first principles effective Hamiltonian [16–19](and refs. therein). Previous PSN simulations [19–21] share some common predictions. *Consistent with experiment*: 1) a first-order $Pm\bar{3}m \rightleftharpoons R3m$ transition to a FE ground-state ($R3m$; $a_0 = 4.080$ *Å*, $\alpha = 89.89°$ at room-T [22]), in both the chemically ordered and disordered states; 2) some broadening of $\epsilon(T)$ in the disordered state; (3) *Apparently* contrary to experiment [8], they all predict that the chemically ordered phase has a higher FE-transition temperature than the chemically disordered phase, $T_{FE}(Ord) > T_{FE}(Dis)$. This result is surprising because in isostructural $Pb(Sc_{1/2}Ta_{1/2})O_3$ (PST) the observed order of transitions is $T_{FE}(Ord) > T_{FE}(Dis)$[23], and one expects the RF in a chemically disordered crystal to depress T_{FE}, as in PST. The unexpected $T_{FE}(Ord) < T_{FE}(Dis)$ result in PSN is partially explained by greater Nb- and/or Sc-displacements in PSN, relative to Ta- and/or Sc-displacements in PST. An effective Hamiltonian simulation that describes PSN ferroelectricity in terms of both Pb- and Nb-modes [21] reduces the difference between $T_{FE}(Ord)$ and $T_{FE}(Dis)$, but does not re-

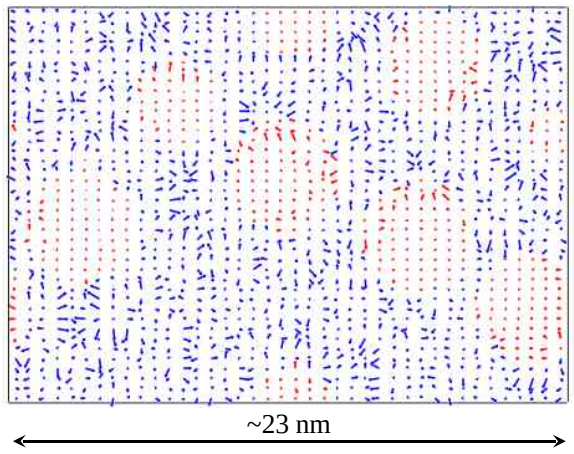

FIG. 1: A (110) plane through the simulation box representing the projected random field (arbitrary units) at each Pb-site that lies in the plane. Chemically ordered regions (approximately circular) have small approximately homogeneous fields, and chemically disordered regions have larger more varied and disordered local fields.

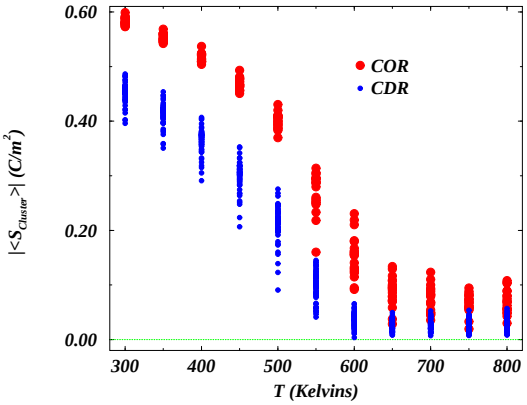

FIG. 2: Average polarizations per unit cell for 800 unit cell clusters, as functions of temperature.

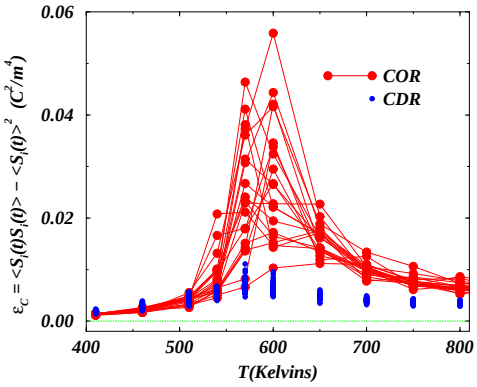

FIG. 3: Polarization fluctuations in chemically ordered and disordered clusters. Lines are for individual ordered clusters.

verse their order. Most likely, however, the $T_{FE}(Ord) < T_{FE}(Dis)$ result is a sample preparation problem: long annealing times are required to achieve a high degree of chemical order, and this promotes Pb-loss, which depresses T_{FE} and yields a more diffuse dielectric peak, as in the Perrin et al. "PSN-85" sample [8].

Chemical order-disorder on the B-sites of $A(B^{3+}_{1/2}B'^{5+}_{1/2})O_3$ and $A(B^{2+}_{1/3}B'^{5+}_{2/3})O_3$ perovskites creates local RF that induce Pb-displacements which presumably cause, or at least contribute to, RFE-properties. Quian and Bursil [12] derived a nearest neighbor (nn) approximation for $\vec{h}$ in $Pb(Mg_{1/3}Nb_{2/3})O_3$ (PMN) and applied it in a two-dimensional Potts-model simulation. A similar three-dimensional model is used here, but the $\vec{h}$ (Fig. 1) are calculated from an electrostatic point-charge model for the full 40^3 B-site configuration, rather than nn B-sites only.

Molecular dynamics (MD) simulations were performed on a first principles effective Hamiltonian model[19] for PSN in a 40^3 unit cell simulation box. Random field terms were combined with an effective Hamiltonian model for a normal FE [16–18] in which all atomic displacements are projected onto a subspace of low-energy FE-distortions, via Pb-centered polar variables. For PSN, this model has the transition temperature defect noted above, but it includes the essential ingredients for a generic RFE model with which to study nano-scale correlations between chemical- and polar-ordering.

The chemical- and therefore RF-microstructure of the simulation box consists of 20 COR in a PDM of 60 CDR. Each COR, and CDR, contains 800 Pb-sites in a convex approximately spherical shape. Figure 1 is a (110) cross section through the simulation box, in which arrows represent $\vec{h}$, proportional to arrow lengths. The COR have relatively low and homogeneous $\vec{h}$, roughly circular projections in Fig. 1. The CDR that make up the PDM have larger more varied $\vec{h}$. In PSN with perfect chemical long-range order, $\vec{h} = 0$ at all Pb-sites, and when B-site disorder is introduced a distribution of RF develops [24]. In a nn approximation for RF [12], $\vec{h} = 0$ at most Pb-sites inside the COR.

Figure 2 plots average COR- and CDR-polarizations, $| < \vec{S}_i(t) > |$, as functions of T: subscript $i = O$ indexes a COR, $i = D$ indexes a CDR, and t is the MD time step. Time averaging is over at least 800 MD snapshots with 100 MD time steps between snapshots (80000 MD steps ≈70 pico seconds). Clearly, the COR exhibit enhanced FE-order over the full T-range. The COR also exhibit enhanced *fluctuations* of individual cluster polarizations, ε_i:

$$\varepsilon_i(T) \equiv < \vec{S}_i(t) \cdot \vec{S}_i(t) > - < \vec{S}_i(t) >< \vec{S}_i(t) > \quad (0.1)$$

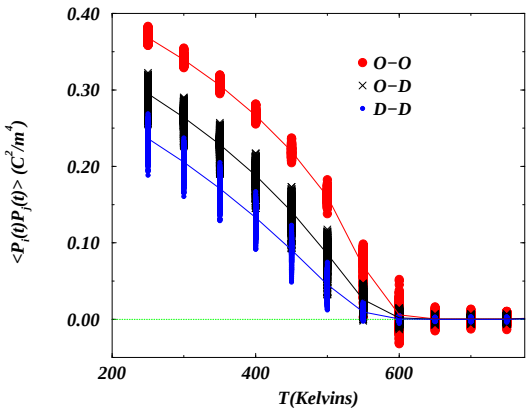

FIG. 4: Cluster-polarization dot products as functions of temperature: O-O indicate products between moments of two chemically ordered clusters, $| < \vec{S}_O(t) \cdot \vec{S}_{O'}(t) > |$; O-D for products between chemically ordered- and disordered clusters, $| < \vec{S}_O(t) \cdot \vec{S}_D(t) > |$; D-D are for two disordered clusters, $| < \vec{S}_D(t) \cdot \vec{S}_{D'}(t) > |$. Solid lines link average products.

which are plotted as functions of T in Fig. 3: $\varepsilon_i(T) \approx$ a local, intra-cluster, dielectric constant. Maxima for, $\varepsilon_O(T)$ curves are two-four times greater than those for $\varepsilon_D(T)$. The, $\varepsilon_O(T)$-maxima occur over a wider range of temperatures, and the normalized widths of $\varepsilon_O(T)$-curves are significantly greater than those for $\varepsilon_D(T)$. Thus, cluster polarizations and their fluctuations are significantly greater in COR, which implies that COR must at least act as nucleii for the PNR.

The prediction of a $Pm\bar{3}m \rightleftharpoons R3m$ FE phase transition is evident in Fig.4 which plots T-dependent dot products of cluster moments, $< \vec{S}_i(t) \cdot \vec{S}_j(t) >$. Solid and dashed lines in Fig.4 connect averages over subsets of the 80 clusters: COR-COR, COR-CDR, and CDR-CDR. Clearly, the model predicts a FE-transition with $T_{FE} \approx 600K$. Below T_{FE}, all three populations [$< \vec{S}_O(t) \cdot \vec{S}_{O'}(t) >$, $< \vec{S}_O(t) \cdot \vec{S}_D(t) >$, and $< \vec{S}_D(t) \cdot \vec{S}_{D'}(t) >$] have *averages* greater than zero which indicates a FE-transition throughout the system. Superficially, this contradicts nuclear magnetic resonance studies of a "20-25%" chemically ordered PSN single crystal by Laguta et al. [25] which indicate that FE-long-range order is clearly stronger in COR than in CDR, but according to Laguta et al. FE long-range order is only established in the COR. However, Laguta et al. also say, "...that even in the disordered parts of the crystal, local polarization acquires a projection along the direction of spontaneous polarization," which is tantamount to acknowledging FE long-range order in the CDR as well. Furthermore, Perrin et. al.[8] report a first-order FE transition in *chemically disordered* PSN. So it appears that the simulations and experiments agree.

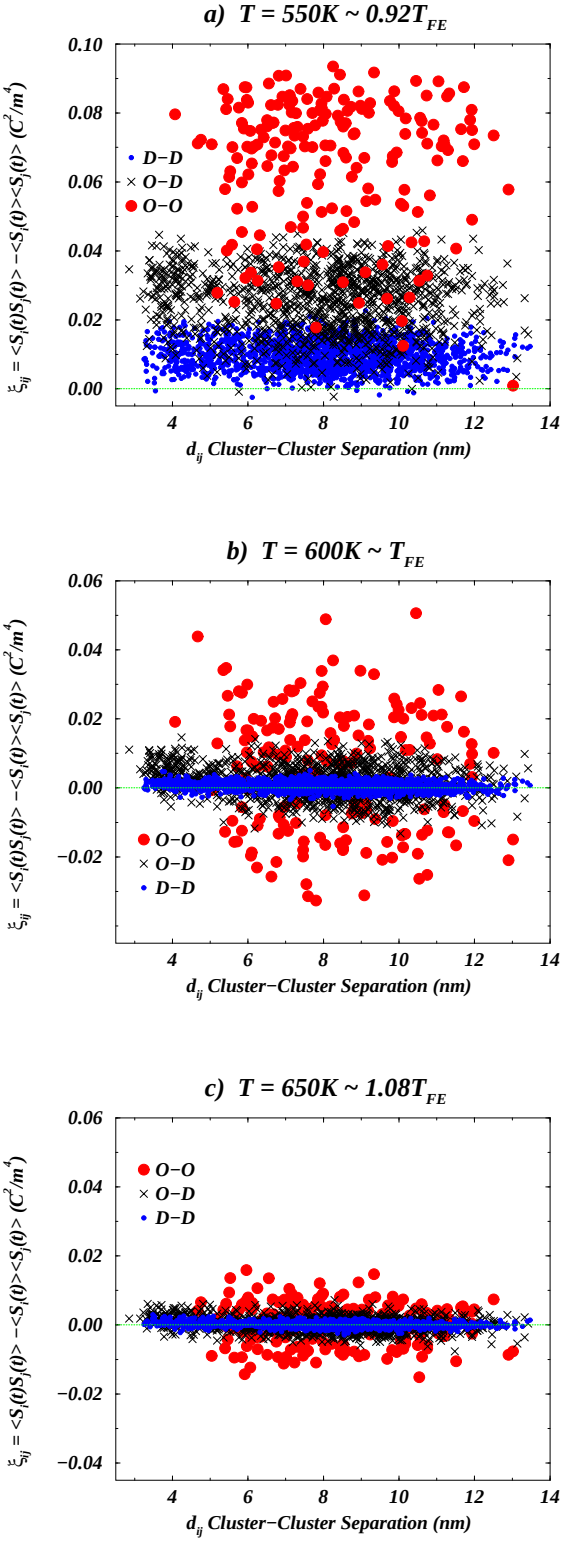

FIG. 5: Isothermal pairwise cluster-cluster correlations as functions of inter-cluster separation d_{ij}: a) $T < T_{FE}$, 550K; b) $T \approx T_{FE} \approx 600K$; c) $T > T_{FE}$, 650K. The magnitudes of pairwise correlations exhibit the hierarchy: $| < \vec{S}_O(t) \cdot \vec{S}_{O'}(t) > | > | < \vec{S}_O(t) \cdot \vec{S}_D(t) > | > | < \vec{S}_D(t) \cdot \vec{S}_{D'}(t) > |$. All figures plotted at the same scale.

The length scale for cluster-cluster separations, d_{ij}, that is sampled in these simulations is $3 \lesssim d_{ij} \lesssim 14nm$ (i and j index O=COR or D=CDR clusters). At this scale, there is no clear d_{ij}-dependence in cluster-cluster *correlations* ξ_{ij},

$$\xi_{ij} \equiv < \vec{S}_i(t) \cdot \vec{S}_j(t) > - < \vec{S}_i(t) >< \vec{S}_j(t) > \qquad (0.2)$$

except perhaps for $d_{ij} \lesssim 6nm$, Figs. 5. Apparently random, d_{ij}-independent, distributions of $\xi_{OO'}$, ξ_{OD}, and $\xi_{DD'}$ above T_{FE} (Figs. 5b and 5c) strongly suggest random-bond type interactions, as postulated in the SRBRFM [15].

The predicted hierarchy of cluster-cluster correlations:

$$|\xi_{OO'}| \; > \; |\xi_{OD}| \; > \; |\xi_{DD'}| \qquad (0.3)$$

implies the spatial mapping COR≈PNR because, at $T_{FE} < T < T_{Burns}$, all the strong correlations are between COR, but none are so strong as to imply multi-COR PNR. A simlation value for T_{Burns}, was not determined, but experimentally, [8] $T_{Burns} \approx 1.1 T_{FE}$ for PSN, consistent with enhanced simulation values for $\varepsilon_O(T)$ above T_{FE}. Therefore, *the characteristic length scale for chemical short-range order is the same as the characteristic length scale for the PNR.*

The pairwise cluster-cluster correlation hierarchy also supports the idea that PNR-PNR interactions are essentially as postulated in the SRBRFM: *effective* PNR-PNR≈COR-COR interactions, $J_{ij} \approx J_{OO'}$, are random; PNR-PDM≈COR-CDR interactions ($\approx J_{OD}$; $|J_{OD}| < |J_{OO'}|$) are significantly weaker than PNR-PNR interactions.

An important difference between the simulations and the phenomenological SRBRFM is that the former include the interactions that drive FE-ordering *within* the COR and PDM: nominally J and J', respectively. In principle, J and J' could be included in SRBRFM calculations, but in practice they have not been[15]. In simulations, J approximately corresponds to the coarce-grained *effective* FE-interaction in chemically ordered PSN, and $J' < J$ is the analogous interaction in the PDM, weakened relative to J by the higher RF-density in the PDM.

Interactions J and J' are significantly stronger in $A(B_{1/2}B'_{1/2})O_3$ systems, hence PSN exhibits a FE-transition even in the chemically disordered state. In $A(B_{1/3}B'_{2/3})O_3$ systems such as PMN, however, J and J' are inherently weaker because of enhanced RF in both COR and CDR: to a first approximation, RF in $A(B_{1/3}B'_{2/3})O_3$ systems are ≈ 1.5 stronger [24] owing to the larger difference in ionic charges, $Mg^{2+} + Nb^{5+}$ in PMN vs. $Sc^{3+} + Nb^{5+}$ in PSN; $A(B_{1/3}B'_{2/3})O_3$ stoichiometry is incompatible with a chemically ordered state in which all $\vec{h} \approx 0$, as in PSN.

Therefore, the random-bond random-field picture is a better approximation for $A(B_{1/3}B'_{2/3})O_3$ systems, such as PMN, which have ferroglass low-T states, than it is for $A(B_{1/2}B'_{1/2})O_3$ systems, such as PSN, which have FE low-T states.

[1] G. A. Smolensky, A. I. Agranovskaya, Sov. Phys. Sol. State **1**, 1429 (1959).
[2] L. E. Cross, Ferroelectrics **76**, 241 (1987).
[3] D. Viehland, S. J. Jang, L. E. Cross and M. Wuttig, J. Appl. Phys. **68**, 2916 (1990).
[4] M. E. Lines and A. M. Glass, *Principles and Applications of Ferroelectrics and Related Materials*, Clarendon Press, Oxford (1979).
[5] A A Bokov, Ferroelectrics, 131, 49 (1992) and A A Bokov, L. A. Shpak and I. P. Raevsky, J Phys Chem Sol 54, 495 (1993).
[6] R. Blinc, V.V. Laguta, and B. Zalar, Phys. Rev. Letters **91**[24] 247601-l (2003).
[7] H.B. Krause, J.M. Cowley and J. Wheatley, Acta. Cryst. **A35** 1015 (1979).
[8] C. Perrin, N. Menguy, O. Bidault, C.Y. Zahara, A.M. Zahara, C. Caranini, B. Hilczer and A. Stepanov, J. Phys. Condens. Matter, **13** 10231 (2001).
[9] H.Z. Jin, J. Zhu, S. Miao, X.W. Zhang, and Z.Y. Cheng J. App. Phys, 89[9] 5048 (2001)
[10] N. Setter and L. E. Cross, J. Appl. Phys. **51**, 4356 (1980).
[11] V. Westphal, W. Kleemann and M. D. Glinchuk, Phys. Rev. Lett. **68**, 847 (1992).
[12] H. Quian and L.A. Bursill, Int. J. of Mod. Phys. **10**, 2027 (1996)
[13] G. Burns and F. H. Dacol Solid State Comm. **48**(10), 853 (1983)
[14] C. A. Randall and A. S. Bhalla, Japn. J. App. Phys. **29**[2], 327 (1990).
[15] R. Pirc and R. Blinc, Phys. Rev **B60**[19], 13470 (1999).
[16] K. M. Rabe and U. V. Waghmare, Phys. Rev. B **52**, 13236 (1995).
[17] U. V. Waghmare and K. M. Rabe, Phys. Rev. B **55**, 6161 (1997).
[18] W. Zhong D. Vanderbilt, and K.M. Rabe Phys. Rev. B. **52**, 6301 (1995).
[19] U.V. Waghmare, E. Cockayne, and B.P. Burton Ferroelectrics **291**, 187 (2003).
[20] R. Hemphill, L. Bellaiche, A. Garcia and D. Vanderbilt Appl. Phys. Lett. **77** 3642 (2000).
[21] E. Cockayne, B.P. Burton and L. Bellaiche, AIP Conf. Proc. 582, 191 (2001) Fundamental Physics of Ferroelectrics 2001, H. Krakauer Ed. Also E. Cockayne, unpublished results.
[22] K. S. Knight and K. Z. Baba-Kishi, Ferroelectrics **173**, 341 (1995).
[23] F. Chu, I.M. Reaney and N. Setter J. Appl. Phys. **77**(4) 1671 (1995).
[24] B.P. Burton, U. V. Waghmare and E. Cockayne, TMS Letters, 1 (2) 29 (2004).
[25] V.V. Laguta, M.D. Glinchuk, I.P. Bykov, R. Blinc and B. Zalar Phys. Rev. **B69**, 054103 (2004).